Assessment of Sochacki lenses for autonomous maritime patrol FLAR

Derek Gray
Department of EEE.,
Xi'an Jiaotong Liverpool University,
Suzhou, Jiangsu, China
derek.gray@xjtlu.edu.cn

Julien Le Kernec
Department of EEE.,
University of Nottingham,
Ningbo, Zhejiang, China
julien.lekernec@nottingham.edu.cn

John Thornton
Antennas Research,
York, Yorkshire, United Kingdom,
john@thorntonj.myzen.co.uk

***Abstract*—Initial numerical and experimental results are given for minimal layer lens antennas for Forward Looking Airborne Radar as the primary sensor onboard small Unmanned Aerial Vehicles adapted for fully autonomous long distance maritime patrol. 27dBi was achieved by a single material lens that is dimensionally compatible with the fuselage of a 6-meter class Unmanned Aerial Vehicle. Numerical results for 2 and 3 layer lenses up to 38dBi directivity were given, been comparable to the reflector antennas presently used in P-3C and P-8A manned maritime patrol aircraft.**

Keywords—FLAR; lens antenna.

I. INTRODUCTION

At present, a cost impediment to the widespread use of mini and small unmanned aerial vehicles (UAVs) is the requirement for those to be continuously monitored by one or more personnel. This class of UAVs have wingspans of 3 to 6 m, Table 1, and are capable of extreme low altitude flying for periods up to 24 hours. Small UAVs have collected data while traversing microbursts and typhoons/cyclones [1, 2], and have collected high resolution photographs of Arctic sea ice melt-ponds [3]. Even when flying fully autonomously under such extreme conditions, continuous human supervision makes those aircraft in effect remotely piloted vehicles. The human supervision can only be removed where there is no need for it; when there is no possible interaction with manned aircraft or adverse terrain, circumventing the practical and legal need for any sense and avoid technology. Long distance maritime flights at low altitude are one such circumstance where existing mini and small UAVs could fly without human supervision, as such flights are by definition over uninhabited open ocean and there is no terrain. Possible civil applications are maritime border patrol, Search and Rescue (SNR), ice patrol and fisheries policing [4]. Specific examples are monitoring Australia's north west maritime border for refugee boats, similar for the Sabah – Mindanao border, and policing the Patagonian Tooth Fish fishery in the Southern Ocean.

Forward Looking Airborne Radar (FLAR) and Side Looking Airborne Radar (SLAR) have a proven history for the above applications, and equivalent systems would be the primary sensor for a maritime specialized small UAV. The US Coast Guard Research and Development Center conducted a series of trials of FLAR and SLAR against life rafts, wooden small craft, fiberglass small craft and ice in the 1980s and 1990s [5, 6]. The detection of 4 to 8-man inflatable life rafts using the AN/APS-137 FLAR was particularly impressive. There are incidental reports of the detection of floating beer cans, which suggests that that radar would have some utility in detection of debris fields [7]. Operator fatigue and overload was noted as a cause of some missed contacts, suggesting the advantage of a fully automated system, such as [8].

TABLE I. SMALL UAV DIMENSIONS

UAV	Wingspan (mm)	Fuselage radius (mm)	Fuselage radius in wavelengths	
			9.5GHz	10GHz
ScanEagle	3,000	90	2.85	3
Aerosonde	2,900	100	3.16	3.3
Aludra	6,000	150	4.75	5

Theoretical assessment of FLAR adapted for existing mass-produced small UAV airframes using a novel, compact and potentially light weight antenna type is the purpose of this work. It is acknowledged that novel and unique airframes can be built around large SLAR systems such has recently been done at Chiba University for a synthetic aperture radar [9], but by not using existent mass-produced airframes defeats the minimal cost concept. The first section of this paper details work to date on a hemispherical lens reflector antenna, while in the last section the performance of FLAR using such an antenna is assessed.

I. SPHERICAL LENS ANTENNAS

A. Existing FLAR antenna and missile antennas

The AN/APS-116 was developed in the 1970s for submarine snorkel and periscope detection [8, 10]. The electronics have been updated several times to be re-designated the AN/APS-127, AN/APS-137 and coastal patrol models [7]. A mechanically steered low mass parabolic dish antenna formed inside a polycarbonate shell was used throughout. The specifications are given in Table 2, from [10].

None of the 3 small UAVs considered have sufficient fuselage radius to encompass the AN/APS-116 antenna, Tables 1 and 2. Taking the 2.4° azimuthal 3dB beamwidth as a primary specification, a circular aperture with a uniform aperture distribution will, by theory, have a radius of 12.3 wavelengths (λ) or 380mm at 9.75GHz, Figure 1 [11]. However, the sidelobe level will be -17.6dB, violating the level set for the AN/APS-116 antenna and make the system more receptive to unwanted signals. In contrast, a circular aperture with a parabola aperture distribution will have a sidelobe level of -24.6dB, but require a radius of 15.3λ or

978-1-4799-4195-7/14/$31.00©2014IEEE

460mm at 9.75GHz for a beamwidth of 2.4°, Figure 1. An optimized Taylor distribution for -20dB sidelobe level will lie between these 2 radii while having an aperture efficiency around 95%, been much higher than the 75% of a parabola distribution [12]. Reducing the radius of the circular aperture to between 2.85 and 5λ as dictated by the fuselage radii of the small UAVs will reduce the antenna gain, broaden the 3dB beamwidth and reduce the FLAR performance and range.

TABLE II. AN/APS-137 AND AN/APY-10 RADAR ANTENNA CHARACTERISTICS

Parameter	AN/APS-137	AN/APY-10
Frequency	9.4 to 10.2 GHz	9.4 to 10.2 GHz
Antenna gain	34.5 dBi	33 dBi
Azimuth beamwidth	2.4°	3.1°
Elevation beamwith	4.0°	4.2°
Azimuth sidelobes	< -20 dB	< -23 dB
Elevation sidelobes	< -20 dB	< -18 dB
Azimuth dimension	1,067 mm	mm
Elevation dimension	610 mm	mm

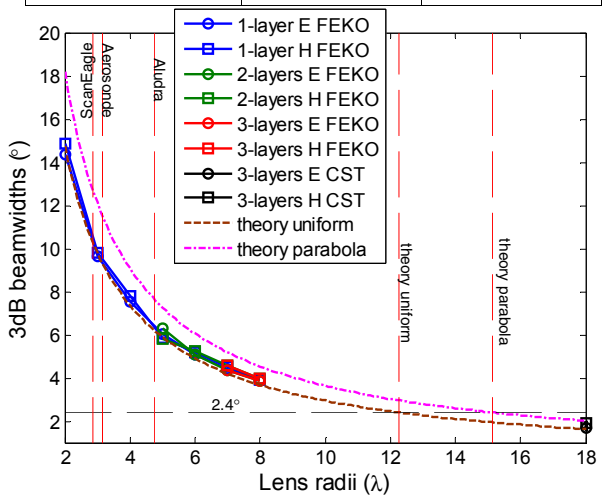

Fig. 1. Theoretical variation of 3dB beamwidths with aperture radius, with numerical beamwidths of spherical lenses with choke feed, from FEKO™; "1-layer" lenses were homogeneous with ε_r=2.3.

The highest possible gain antenna for a FLAR system in the nose of a small UAV will have to exploit as much of the fuselage radius as possible. Under these constraints, the history of missile nose antennas is more relevant than that of manned aircraft. One approach is to fill the entire radius of the fuselage with a horn antenna, and mechanically scan the Gaussian beam by spinning 2 or 3 wedge shaped slow-wave platters [13]. Despite the attractive mechanical simplicity of this design, the scan performance and limitations are unknown. A derivative dielectric wedge design only scanned across ±16°, however more recent work employing microstrip structure achieved scan to 60° at the cost of 3dB scan loss, but at the relatively low gain of 27.8dBi [15]. Another approach is to fill the radius of the fuselage with a Luneburg lens antenna, which has the unique advantage of producing identical beams irrespective of beam pointing angle [16]. A more conventional alternative to the receive-only microwave optical transducers of [16] is to rotate a single TRM with an appropriate small scalar feed antenna on a gimbal behind the lens antenna, which has the advantage of reduced mass in motion and consequent minimized moment. Novel gimbals were developed for ground station Luneburg lens antennas for the proposed LEO satellite system Skybridge™ [17] and high speed train to satellite antenna [18]. Another possible lens antenna configuration involves a static scalar feed antenna while a hemispherical lens on a reflecting plate is rotated by gimbal [19]. This configuration was investigated for Q-band airliner to ground data link and was found to be capable of the required 92° scan range [20, 21]. Two different lens antenna configurations are thus possible and are sketched in Figure 2, but the development of either is dependent on the reduction of both Luneburg lens antenna mass and cost.

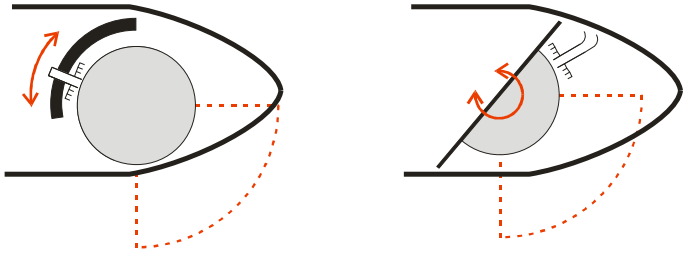

Fig. 2. Sketch of nose mounted lens antenna configurations; spherical lens with feed antenna and TRM on gimbal, stationary feed antenna with gimballed hemispherical lens reflector.

The ceramic powder doped foams developed for the Skybridge™ antennas and derivative products significantly reduced the mass of spherical or hemispherical Luneburg lens antennas [17, 22]. Theoretically, a Luneburg lenses has a continuous variation in relative permittivity (ε_r) from 2 at the center of the spherical lens to 1 at the surface. The continuous curve is approximated by discrete steps in ε_r realized by a series of 10 or more nested hemispherical shells each molded from a different ceramic powder loaded foam. Reducing the number of hemispherical shells will reduce the cost of production; lesser number of mated molds, unique materials, parts for assembly and construction failures due to air gaps between layers.

A single material (1-layer) homogeneous spherical lens is obviously the simplest possible structure, and have been demonstrated as practical antennas in the past [23, 24]. The ε_r used will determine the focal length and the choice of optimal scalar feed antenna for lens radii up to about 6λ or 31dBi [20, 25]; there is no need to use a Luneburg lens when a homogeneous lens will suffice. Given that the fuselage radii of the ScanEagle and Aerosonde UAVs are below 4λ, homogeneous lenses will suffice.

A series of numerical simulations of ε_r=2.3 spherical lenses were run in the commercially available software FEKO™ and a custom SWE code, which has a considerable processing speed advantage over the former [25]. The lens radius was varied from 2 to 6λ for the FEKO™ models, whereas 2 to 14λ was run in the SWE code. The characteristics of the feed

antennas for either simulation model are specified in Table 3. The differences in feed beamwidth prevent a direct comparison between the 2 simulation types; the 2-dipole feed of the SWE models tends to over-illuminate the lenses, as noted in [26] where high sidelobe levels were obtained. For both simulation types, the feed was moved along a radial line until the maximum directivity was found.

TABLE III. CHARACTERISTICS OF FEEDS FOR LENSES

Antenna	Directivity (dBi)	E-plane 3dB beamwidth (°)	H-plane 3dB beamwidth (°)
2 dipole SWE	5	72	165
Choked FEKO™	9.1	66.2	73.5
Choked CST™	9.8	64	66

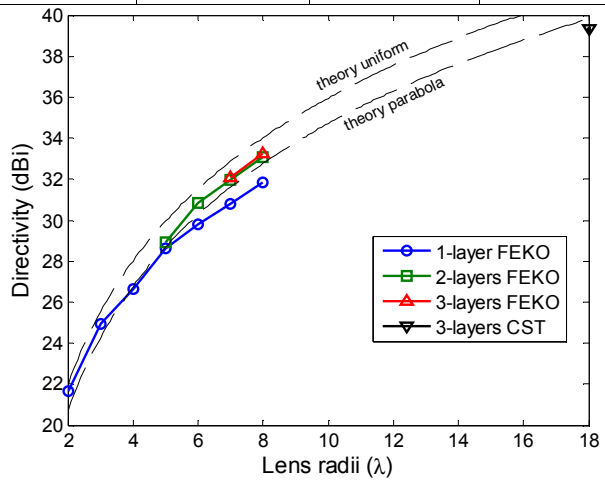

Fig. 3. Directivity of numerical simulated spherical lenses with choked feeds, from FEKO™ and CST™; "theory parabola" has 75% aperture efficiency.

Considering the FEKO™ simulations of ε_r=2.3 1-layer spherical lenses, the directivity increased steadily with increasing radius, Figure 3. This directivity increase, however, did not match the rate of increase that would be expected of an increasing circular aperture over which the aperture distribution is held constant; the aperture efficiency was found to decrease with increasing lens radius, Figure 4. The SWE simulations gave an identical trend, although with 10% higher aperture efficiencies. Checking the 3dB beamwidths, those stayed consistent with what was expected theoretically from a circular aperture having a uniform aperture distribution, indicating that the beamwidths are close to optimal [14], Figure 1. Examining the sidelobe levels, Figure 5, the overall trend was for the sidelobe levels to increase with increasing lens radius, and as the sidelobe levels increased, less power was available for the main lobe and the rate of directivity increase with increasing lens radius falls off. It is speculated that the aperture distribution of the scalar feed antenna needs to be scaled with increasing lens radius. The optimal feed position for highest lens directivity was found to increase with increasing lens radius, Figure 6.

An approximately 3λ radius ε_r=2.3 lens fits the fuselage dimensions of the 3 meter class small UAVs, ScanEagle and Aerosonde. Compared to the reflector antennas used in the AN/APS-137 and AN/APY-10 radar, there would be approximately a 10dB decrease in antenna gain. The consequences of this on detection range are considered in Section 3.

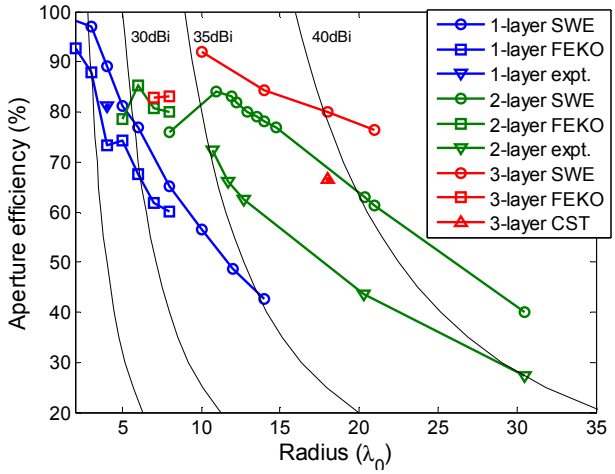

Fig. 4. Aperture efficiencies of 1 to 3-layer spherical lenses, from SWE code, FEKO™, CST™ and experiement.

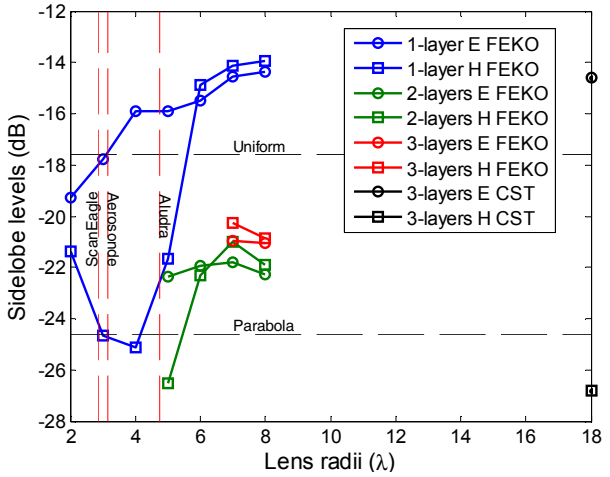

Fig. 5. Sidelobe levels of spherical lenses with choke feed, from FEKO™.

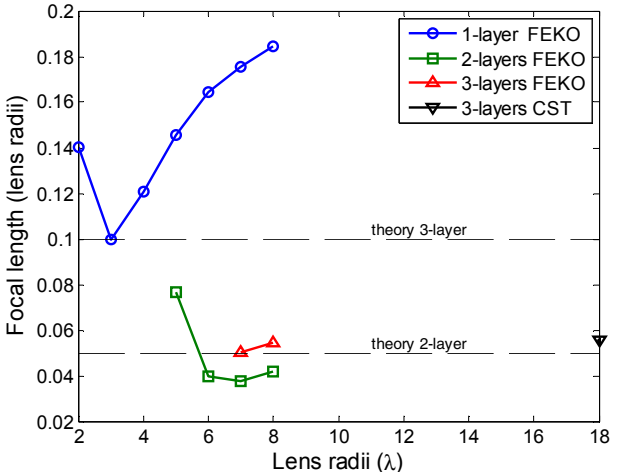

Fig. 6. Focal lengths of numerical simulated spherical lenses with choked feeds, from FEKO™ and CST™.

B. Sochacki lens antennas

For lens radii beyond 6λ, it has been found that a second inner layer should be added [25]. A numerically optimized 2-layer was found to be consistent with graded index media theory [26]. The same theoretical work showed that Luneburg lenses are a limiting case having ε_r=1 of the lens surface [27]. If some minor surface reflection can be tolerated, then the variation of ε_r between lens center and surface can be minimized, which in turn decreases the number of discrete hemispherical shells needed to approximate that curve, reducing manufacturer costs. Here, the work that was started in [25] with polyethylene (ε_r=2.3; PE) and cross-linked polystyrene/Rexolite (ε_r=2.53; xPS) is continued.

The optimal proportional radius of a sphere of xPS within a PE spherical outer layer was found to be 0.47 [25]. This 2-layer lens design was run in FEKO™, with the radius was varied from 5 to 8λ. The 3dB beamwidths were consistent with those expected of a circular aperture with a uniform aperture distribution, Figure 1. The directivity was higher and increased with more consistently with radius than that of the 1-layer ε_r=2.3 lenses, Figure 3. However, the aperture efficiency still decreased with increasing lens radius, Figure 4. This trend was consistent with the previously reported SWE and experimental results [26]. The sidelobe levels were reasonably stable around -22dB below peak and thus been satisfactory for the FLAR application, Figure 5. The focal length used in the Sochacki equation to match the xPS – PE discrete layer lens design was 0.05 lens radii [26]. The optimal position for the choked feed was 0.04 lens radii from the lens surface to the mouth of the choked feed, with the difference from 0.05 likely been the result of the feed phase center been inside the mouth of the circular waveguide of the choked feed, Figure 6.

At this preliminary stage, it is difficult to recommend either a 1-layer or 2-layer lens for a 6 meter class small UAV such as Aludra. Given the relative behavior of the 1-layer and 2-layer lenses for around 5λ radius, there will be a design compromise between scalar feed design sophistication against cost of adding the inner xPS layer.

To approach or exceed the gain of the reflector antennas used in the AN/APS-137 and AN/APY-10 radar, an intermediate layer would need to be added between the inner xPS sphere and the outer PE layer, as the discretized 2-layer lens has diverged too much from the continuous relative permittivity curve. Cross-linked polyethylene (xPE) has ε_r=2.4, and is thus suitable as an intermediate layer [26]. Discretizing the Sochacki curve into 3 steps gave an inner xPS sphere of 0.37 of the total radius and a xPE spherical shell layer of outer radius 0.55 of the total encased within an outer layer of PE. This design was run in the SWE code and the commercially available codes FEKO™ (MLFMM solver) and CST™ (integral equation solver). Radii of 10 to 21λ were run in SWE, and showed some 5 to 15% higher aperture efficiencies over the 2-layer design run in the same code, Figure 4. For a radius of 8λ, the FEKO™ results showed a 5% increase over the aperture efficiency of the 2-layer design run in FEKO™, suggesting that at this radius transitioning to the 3-layer design will be worthwhile; although there was little change in the 3dB beamwidth and sidelobe level, Figures 1 and 5. The 3dB beamwidth of the 18λ lens run in CST™ was likewise comparable to that of a uniformly illuminated aperture, Figures 1 and 7. The focal length used in the Sochacki equation was 0.1 lens radii, but the FEKO™ 8λ lens and the CST™ 18λ lens both gave optimal feed positions of 0.55, Figure 6; which will be investigated in the future.

The 3-layer CST™ 18λ lens had a directivity of 39.3dBi, which exceeds the gains of the AN/APS-137 and AN/APY-10 antennas, Table 2. As an initial design this was considered satisfactory. The next step is to reduce the -14.5dB E-plane sidelobe by minor modifications to the choked feed, Figures 5 and 7. Once that is achieved, the E-plane beamwidth will be broadened to 4° in the vertical plane to give an improved footprint. Any minor reduction of lens radius could then be considered. As the design stands, the radius is 480mm which exceeds the fuselage of the 6-meter class Aludra UAV, Table 1. Consequently, if the AN/APS-137 and AN/APY-10 is to be matched, a custom wide body fuselage is required.

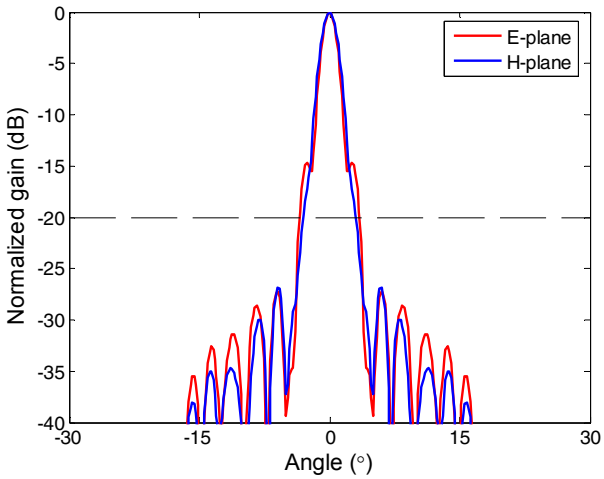

Fig. 7. Radiation pattern of 3-layer 18λ radius spherical lens, from CST™.

C. Prototype single layer antenna

With the experimental apparatus available from [21], a 4λ PE hemispherical lens reflector was built and tested, Figure 8. This lens would dimensionally fit within the nose of the 6 meter class Aludra UAV. The hemispherical lens was machined from a cylindrical billet of ultra high molecular weight polyethylene (UHMW-PE) provided by Saxin Corporation. The jig used only allowed for rotation in what would be the elevation plane when installed in the aircraft, Figures 2 and 8.

With the scan angle set to 90°, the choked feed was moved on tracks along a radial line to find the optimal received gain. The peak received gain was found to be at a separation of 0.13 lens radii, Figure 9. The measured gain differences between E_h and E_v were within experimental error. The E_h component would correspond to vertical linear when installed in an aircraft. It was noticed during this exercise that the sidelobe levels were also affected by feed to lens separation. A separation of 0.2 lens radii gave -20dB sidelobes for the E_h component, Figure 10. The scan performance of this antenna

will be measured during future work, followed by feed antenna design optimization.

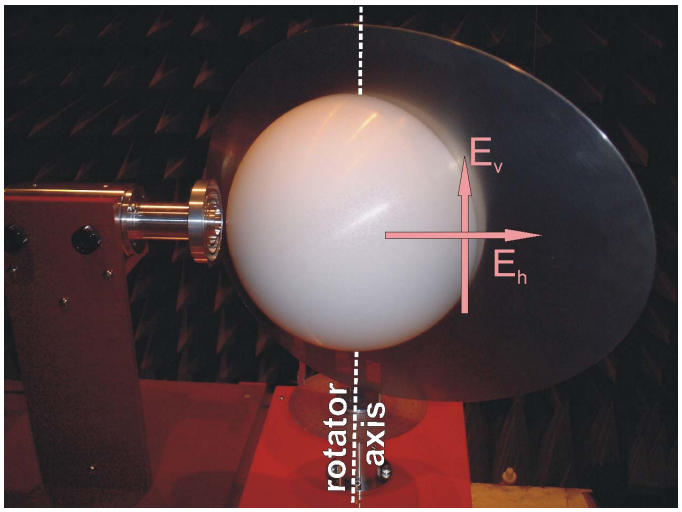

Fig. 8. Photograph of choked feed, 4λ radius UHMW-PE lens and jig.

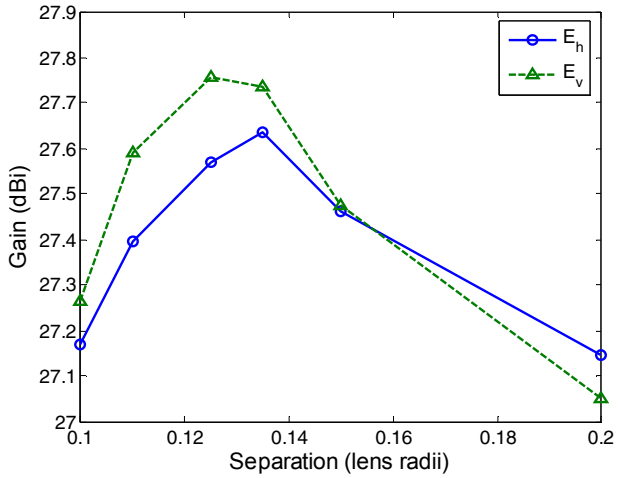

Fig. 9. Measured gain variation of 4λ radius UHMW-PE lens with separation from lens surface.

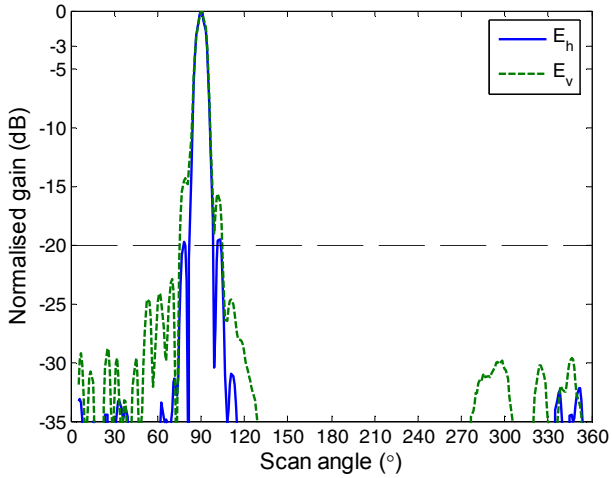

Fig. 10. Measured radiation patterns of 4λ radius UHMW-PE lens.

II. FLAR Radar Performance Assessment

As an initial assessment of the consequences of changing from the AN/APS-137 or AN/APY-10 onboard a manned aircraft to a system carried by a small UAV, an analysis of detection range reduction resulting from the use of physically smaller antennas was done. It was assumed that all the terms of the monostatic radar equation were identical except for the antenna gain. The estimated gain/loss in maximum detection range compared to AN/APY-10 for the proposed lens antennas at 9.5GHz with characteristics as summarized in Table 4 is shown in Figure 11.

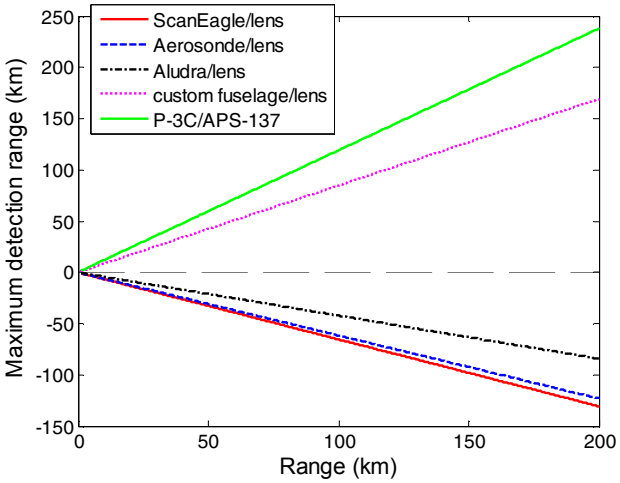

Fig. 11. Estimated gain/loss in maximum detection range with featured antennas compared to APY-10 at 9.5GHz.

The estimated maximum detection range ratio compared to the AN/APY-10 at 9.5GHz are given in Table 5. This for a submarine snorkel (1dBsqm) at 53km for the AN/APY-10, and should be indicative of other small targets such as wooden boats and inflatable life rafts.

TABLE IV. Estimated Radar Antenna Characteristics

Radar denomination	Antenna radius (mm)	Antenna gain (dBi)	Beamwidths		FOV (°)
			azimuth	elevation	
APS-137 on P-3C	534 x 305	34.5	2.4	4	±105
APY-10 on P-8A	n/a	33	3.1	4.2	±120
ScanEagle	90	23	12.8	12.8	n/a
Aerosonde	100	24	12.1	12.1	n/a
Aludra	150	28	11.5	11.5	n/a
Custom wide body fuselage	480	38	2.4	2.4	n/a

III. CONCLUSIONS

Homogeneous and Sochacki lenses were considered as FLAR antennas for small UAVs. The former type is appropriate for the 3-meter class UAVs, while a 2-layer Sochacki lens may prove best for a 6-meter class UAV. If the characteristics of the systems presently used onboard manned aircraft are to be matched, a custom UAV with approximately 1 meter diameter fuselage is required. Future economic modelling is required to assess the benefits of small UAVs for long duration maritime patrol over manned aircraft. The transition radii at which a change from 2-layer to 3-layer Sochacki lens when increasing aperture size were further elucidated; been about 8λ.

TABLE V. ESTIMATED CHARACTERISTICS RELATIVE TO APY-10 AT 9.5GHZ

Aircraft	Antenna	Maximum detection range ratio (%)	1dBsqm target maximum range (km)
P-3C	reflector	118.9%	63
ScanEagle	lens	34.7%	18.4
Aerosonde	lens	38.5%	20.4
Aludra	lens	57.9%	30.7
Custom fuselage	lens	184.9%	97.8

ACKNOWLEDGMENT

The authors wish to thank Dr. Peter Wittenberg of Boeing for a vigorous debate on the economics of UAVs at the 2013 IET Radar conference, which inspired this work. The experimental results reported in this paper were measured at the Kashima Space Centre during the 2008/2009 financial year and were sponsored by the Ministry of Infrastructure and Communications of the Government of Japan. The authors also wish to thank Dr. Fujino of Toyo University, and Dr. Orikasa and Mr. Korumo of NICT for their assistance in the preparation for the experimental work. Likewise, the authors acknowledge and thank EMSS SA for providing an academic license of FEKO™.

REFERENCES

[1] G.J. Holland, P.J. Webster, J.A. Curry, G. Tyrell, D. Gauntlett, G. Brett, J. Becker, R. Hoag & W. Vaglienti, "The aerosonde robotic aircraft: a new paradigm for environmental observations," *Bulletin of the American Meteorological Society*, pp. 889-901, May 2001.

[2] P.-H. Lin, "The first successful typhoon eyewall-penetration reconnaissance flight mission conducted by the unmanned aerial vehicle, aerosonde," *Bulletin of the American Meteorological Society*, pp. 1481-1483, Nov. 2006.

[3] J. Inoue, J.A. Curry & J.A. Maslanik, "Application of aerosondes to melt-pond observations over arctic sea ice," *Bulletin of the American Meteorological Society*, pp. 327-334, Feb. 2008.

[4] T.H. Cox, C.J. Nagy, M.A. Skoog & I.A. Somers, "Civil UAV capability assessment," *NASA Dryden Flight Research Center*, December 2004.

[5] R.Q. Robe, N.C. Edwards, D.L. Murphy, N. Thayer, G.L. Hover & M.E. Kop, "Evaluation of surface craft and ice target detection preformance by the AN/APS-135 side-looking airbourne radar (SLAR)," *U.S. Dept. of Transportation United States Coast Guard*, Report CG-D-2-86, December 1985.

[6] R.Q. Robe, D.L. Raunig & R.L. Marsee, "AN/APS-137 forward looking airbourne radar (FLAR) evaluation final report," *U.S. Dept. of Transportation United States Coast Guard*, Report CG-D-18-94, May 1994.

[7] N. Friedman, "The Naval Institute Guide to World Naval Weapon Systems," *Naval Institute Press*, 1997 & 2006.

[8] J.J. Ousborne, D. Griffith & R.W. Yuan, "A Periscope Detection Radar," *Johns Hopkins APL Technical Digest*, vol. 18, num. 1, 1997.

[9] J.T.S. Sumantyo & K.V. Chet, "Development of Synthetic Aperture Radar onboard unmanned aerial vehicle," *2013 Asia-Pacific Conference on Synthetic Aperture Radar (APSAR)*, 2013, pp. 37 – 40.

[10] J.M. Smith & R.H. Logan, "AN/APS-116 periscope-detecting radar," *IEEE Transactions on Aerospace and Electronic Systems*, vol. AES-16, iss. 1, Jan. 1980, pp. 66 – 73.

[11] Chapter 5 in "Antenna Handbook," Editors Y.T. Lo, S.W. Lee. Springer, 1988.

[12] R.C. Rudduck, D.C.F. Wu & R.F. Hyneman, "Directive Gain of Circular Taylor Patterns," *Radio Science*, 1971, vol. 6(12), pp. 1117–1121.

[13] R.W. Sandoz & M.M. Rosenthal, "Rotating lens antenna seeker-head", *United States patent 3,979,755*, September 7, 1976.

[14] M.R. Khan, "A beam steering technique using dielectric wedges," PhD thesis, University College London, December 1985.

[15] N. Gagnon & A. Petosa, "Using rotatable planar phase shifting surfaces to steer a high-gain beam," *IEEE Trans. on Antennas and Prop.*, vol. 61, no. 6, June 2013, pp. 3086-3092.

[16] D.P. Hilliard & D.L. Mensa, "Photonic electromagnetic field sensor for use in a missile," *United States patent 5,384,458*, Jan. 24, 1995.

[17] T. Ogawa, "Antenna apparatus", *United States patent 6,380,904*, April 30, 2002.

[18] J. Thornton, S. Gregson & D. Gray, "Aperture Blockage and Truncation in Scanning Lens-Reflector Antennas", *IET Microwaves, Antennas & Propagation*, vol. 4, iss. 7, July 2010, pp. 828-836.

[19] P.N. Migdal, "Steerable radar antenna", *United States patent 3,848,255*, November 12, 1974.

[20] D. Gray, J. Thornton, H. Tsuji & Y. Fujino, "Scalar feeds for 8 wavelength diameter homogeneous lenses", *IEEE Antennas and Propagation Symposium Digest, North Charleston*, June 2009, paper 429.6.

[21] D. Gray & J. Thornton, "Scan Performance of Low Index Lens Reflector," *IET International Radar Conference 2013*, Xi'an, April 2013, paper G0470.

[22] T. Hatsuda, et al., "Unique Attenuation Characteristics of Ku-Band Lune-Q Antenna for Satellite Re-Transmission of Terrestrial Digital Broadcasting Signal," *2007 IEEE Antennas Propag Symposium.*, June 2007, paper 209.6.

[23] T. Ap Rhys, "The homogeneous sphere as a millimeter-wave lens", *1966 IEEE International Antennas and Propagation Symposium*, Dec 1966, pp. 59-66.

[24] W. Williams, "Advanced Lightweight Electronically Steered Antennas for Responsive Space Payloads", *AIAA-LA Section 1st Responsive Space Conference*, Redondo Beach, CA, April 1–3, 2003, pp 1-10.

[25] J. Thornton, "Wide-scanning multi-layer hemisphere lens antenna for Ka band", *IEE Proc.-Microw. Antennas Propag.*, Vol. 153, No. 6, December 2006.

[26] D. Gray, J. Thornton & R. Suzuki, "Assessment of discretised Sochacki lenses", *LAPC 2009 Loughborough Antennas & Propagation Conference*, Nov. 2009, pp. 297 – 300.

[27] J. Sochacki, F.R. Flores and C. Gómez-Reino, "New method for designing the stigmatically imaging gradient-index lenses of spherical symmetry," *Applied Optics*, vol. 31, no. 25, Sept. 1992, pp. 5178-5183.